Analytic control of jet substructure

Laís Schunk

IPhT - CEA Saclay

Work being finalized with Gregory Soyez and Mirinal Dasgupta

November 19, 2015

Presentation plan

Presentation plan

Introduction

- QCD partons in high energies (LHC) can not be directly observed and their final state are complex structures called *jets*;

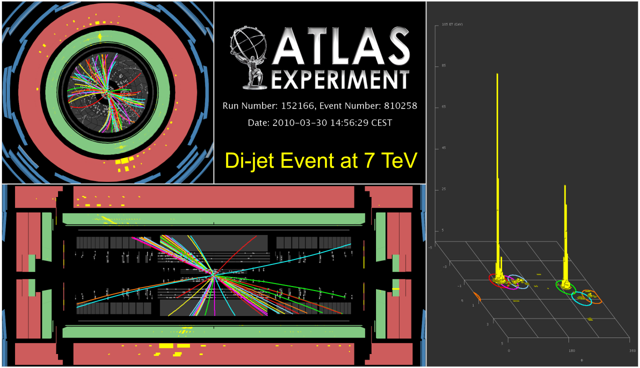

ATLAS collaboration

- Jets are used very frequently in LHC analysis.

Definition of jet

- A *jet definition* is a set of rules to cluster particles into jets;
- Composed of a *recombination algorithm* and its *parameters* (usually the jet radius R);

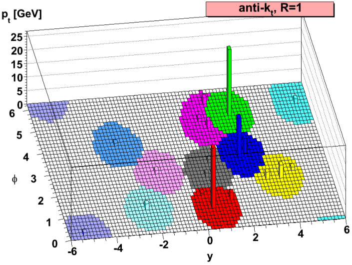

M. Cacciari, G. P. Salam and G. Soyez (2008)

- LHC uses the anti-k_t algorithm.

Presentation plan

Boosted heavy particles

- At the LHC $\rightarrow$ boosted ($p_t \gg m$) heavy particles
  $\rightarrow$ decay in very collimated final states
  $\rightarrow$ clustered into a single jet;

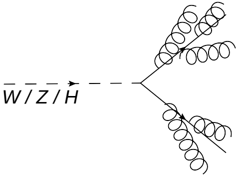

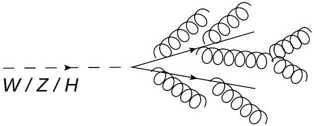

- Characteristic opening angle of the jet is $\theta \propto \dfrac{m}{p_t}$.

QCD background

- QCD collinear divergences keep parton jets collimated for any p_t;

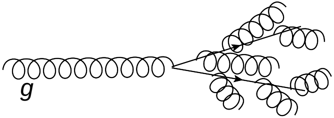

QCD background

- QCD collinear divergences keep parton jets collimated for any p_t;

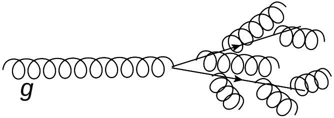

How to discriminate QCD jets from $Z/W/H \to hadrons$ jets?

QCD background

- QCD collinear divergences keep parton jets collimated for any p_t;

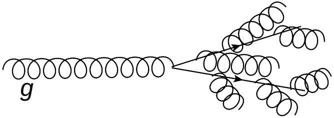

How to discriminate QCD jets from $Z/W/H \rightarrow hadrons$ jets?

Possible method : partons are *color charged particles*, they produce different radiation patterns from bosons.

Jet substructure

- Knowing the mass of a jet is not enough to identify its origin, we need to access the *jet substructure* ;

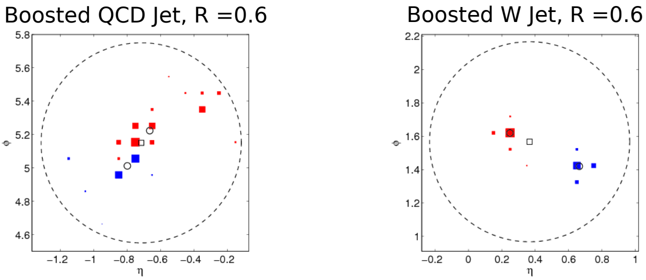

J. Thaler and K. V. Tilburg (2010)

- Different techniques are available:
  1. Find hard cores (1 for QCD, 2 for bosons);
  2. Constrain the radiation patterns.

Application : diboson excess

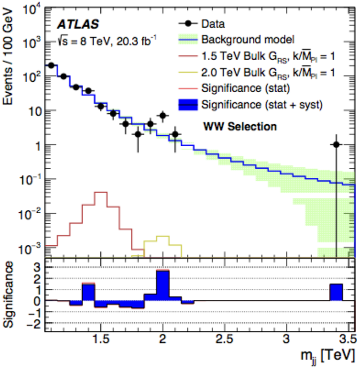

ATLAS collaboration

- ATLAS found a 3.2σ excess in diboson resonances at $\sim 2 TeV$;
- CMS found similar anomalies;
- High energy events $\rightarrow$ very collimated final states.

Presentation plan

Control of jet substructure

- *Constraint radiation patterns to discriminate different types of jets;*
- Making use of jet-shapes : observables that are functions of the jet constituents $v(p_1^\mu, p_2^\mu, ..., p_n^\mu)$;
- In this work we chose $v = \tau_{21}$, μ^2 and C_2 (next slide);
- Understand differences/similarities from a *first-principle analytical study*.

Jet shapes (angular parameter $\beta = 2$)

- **Energy correlation**

$$C_2^{(2)} = e_3^{(2)}/(e_2^{(2)})^2,$$

$$e_2^{\beta} = \frac{1}{p_t^2 R^{\beta}} \sum_{i<j\in jet} p_{t,i} p_{t,j} \theta_{ij}^{\beta},$$

$$e_3^{\beta} = \frac{1}{p_t^3 R^{3\beta}} \sum_{i<j<k\in jet} p_{t,i} p_{t,j} p_{t,k} \theta_{ij}^{\beta} \theta_{ik}^{\beta} \theta_{jk}^{\beta}.$$

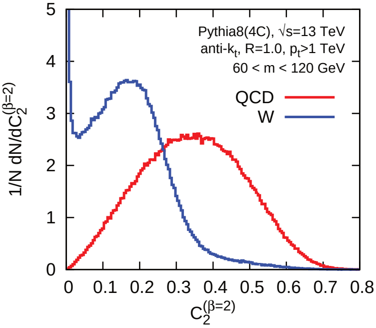

Jet shapes (angular parameter $\beta = 2$)

- **N-subjettiness** with axes $a_1, ..., a_N$

$$\tau_{21}^{(2)} = \frac{\tau_2^{(2)}}{\tau_1^{(2)}}, \qquad \tau_N^\beta = \frac{1}{p_{t,jet} R^\beta} \sum_{i \in jet} p_{t,i} \min_{a_i \dots a_N} (\theta_{ia_1}^\beta, ..., \theta_{ia_N}^\beta).$$

- **Mass-drop** with subjets j_1 and j_2

$$\mu_p^2 = \max(m_{j1}^2, m_{j2}^2)/m_j^2.$$

Lund diagrams

- We consider boosted jets of a *given mass*, $\rho = m^2/p_t^2 R^2 \ll 1$;
- Lund diagram : graphical representation of the results in $z\theta$ vs. $1/\theta^2$ coordinates.

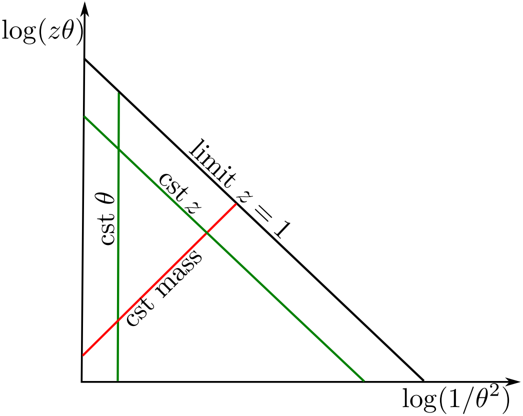

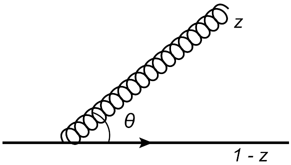

- We consider boosted jets of a *given mass*, $\rho = m^2/p_t^2 R^2 \ll 1$;
- Lund diagram : graphical representation of the results in $z\theta$ vs. $1/\theta^2$ coordinates.

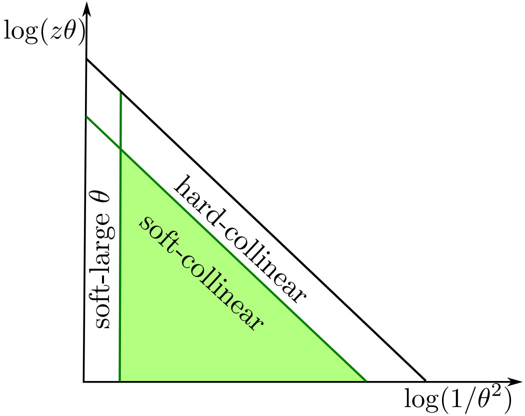

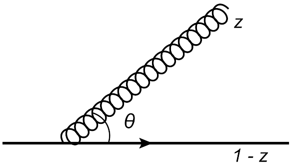

Structure of the results (QCD background)

- Up to LL, emissions are strongly ordered in mass and angle.
- Independent emissions → constraints as an exponential factor.
- For a jet of a given mass:

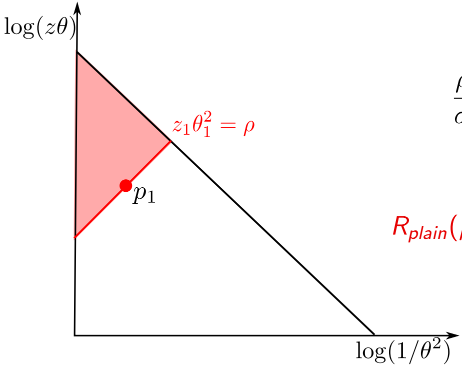

$$\frac{\rho}{\sigma}\frac{d\sigma}{d\rho} = \int_\rho^1 dz_1 P_i(z_1)\frac{\alpha_s}{2\pi}e^{-R_{plain}(\rho)}$$

$$R_{plain}(\rho) = \int_0^1 \frac{d\theta^2}{\theta^2}\int_0^1 dz P_i(z)\frac{\alpha_s}{2\pi}\Theta(z\theta^2 > \rho)$$

Structure of the results (QCD background)

- For a jet of a given mass + a cut in the shape $v_{cut} \ll 1$:

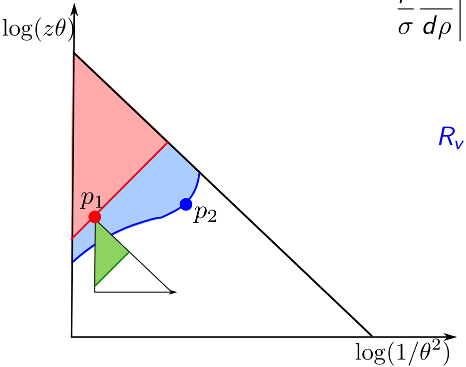

$$\frac{\rho}{\sigma}\frac{d\sigma}{d\rho}\Big|_{<v} = \int_\rho^1 dz_1 P(z_1)\frac{\alpha_s}{2\pi} e^{-R_{plain}(\rho)-R_v(\rho,z_1)}$$

$$R_v(\rho,z_1) = \int_0^1 \frac{d\theta_2^2}{\theta_2^2}\int_0^1 dz_2 P_i(z_2)\frac{\alpha_s}{2\pi} \times\Theta(v>v_{cut})\Theta(z_2\theta_2^2<\rho) + \int_0^1 \frac{d\theta_{12}^2}{\theta_{12}^2}\int_0^1 dz_2 P_g(z_2)\frac{\alpha_s}{2\pi} \times\Theta(v^{sec}>v_{cut})$$

Structure of the results (QCD background)

- For a jet of a given mass + a cut in the shape $v_{cut} \ll 1$:

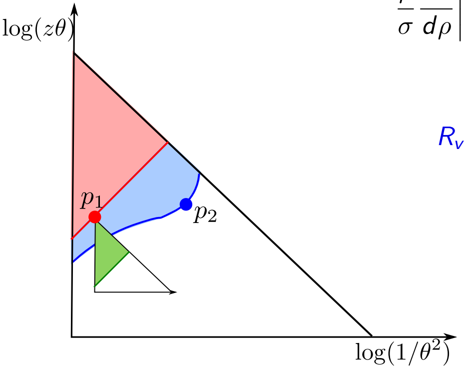

$$\frac{\rho}{\sigma}\frac{d\sigma}{d\rho}\bigg|_{<v} = \int_\rho^1 dz_1 P(z_1)\frac{\alpha_s}{2\pi} e^{-R_{plain}(\rho) - R_v(\rho, z_1)}$$

$$R_v(\rho, z_1) = \int_0^1 \frac{d\theta_2^2}{\theta_2^2}\int_0^1 dz_2 P_i(z_2)\frac{\alpha_s}{2\pi} \times\Theta(v > v_{cut})\Theta(z_2\theta_2^2 < \rho) + \int_0^1 \frac{d\theta_{12}^2}{\theta_{12}^2}\int_0^1 dz_2 P_g(z_2)\frac{\alpha_s}{2\pi} \times\Theta(v^{sec} > v_{cut})$$

Now all we need is to find $v(\rho, z_1, z_2, \theta_2)$.

N-subjettiness	*Mass drop*	*Energy correlation*

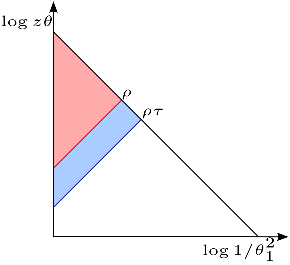

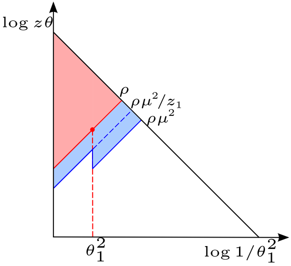

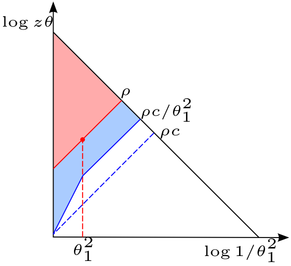

$$R_\tau(z_1) = \frac{\alpha_s C_R}{2\pi}\left[\frac{L_\tau^2}{2} + L_\rho L_\tau\right] + \frac{\alpha_s C_A}{2\pi}\frac{L_\tau^2}{2}$$

$$R_{\mu^2_{1/2}}(z_1) = \frac{\alpha_s C_R}{2\pi}\left[\frac{L_\mu^2}{2} + L_\rho L_\mu\right] - \frac{\alpha_s C_R}{2\pi}\frac{L_1}{2}(L_\rho - L_1) + \frac{\alpha_s C_A}{2\pi}\frac{(L_\mu - L_1)^2}{2}$$

$$R_{C^2}(z_1) = \frac{\alpha_s C_R}{2\pi}\left[\frac{L_e^2}{2} + (L_e - L_\rho + L_1)L_1\right] + \frac{\alpha_s C_A}{2\pi}\frac{1}{2}(L_e - L_\rho + L_1)^2$$

$$L_X = \log(1/X)$$

ROC curves

- Probability that $v_{QCD} < v_{cut}$ vs. probability that $v_{sig} < v_{cut}$;
- C_2 is the most efficient, and τ_{21} more efficient than μ^2 (more delicate call).

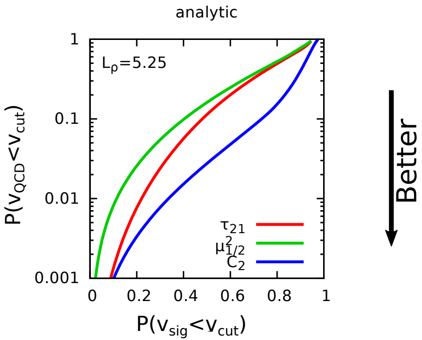

ROC curves

- Probability that $v_{QCD} < v_{cut}$ vs. probability that $v_{sig} < v_{cut}$;
- C_2 is the most efficient, and τ_{21} more efficient than μ^2 (more delicate call).

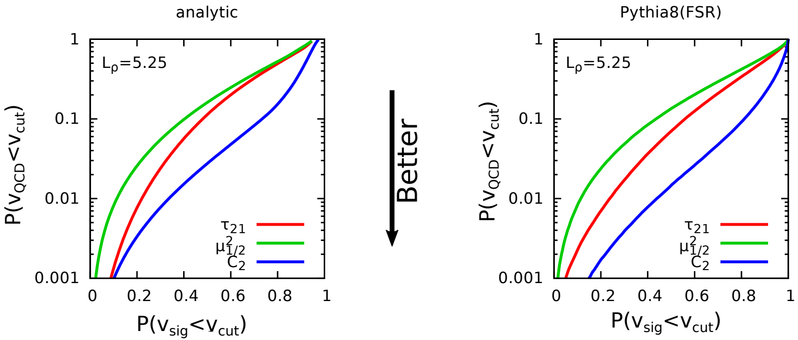

- Good description of the order between shapes.

Presentation plan

Conclusion

- Good **qualitative description** of the shapes.
- **Efficiency** of the shapes: $C_2 > \tau_{21} \gtrsim \mu^2$.
- **Future works**
  - Add grooming (in progress);
  - Higher accuracy (in progress);
  - Different jet shapes (next);
  - 3-pronged jet shapes;
  - ISR contributions;
  - Calculations for finite v.

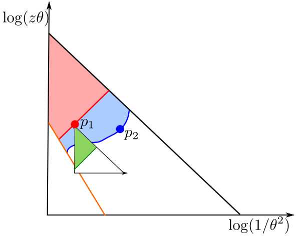

Backup Slides

Diboson excess at CMS

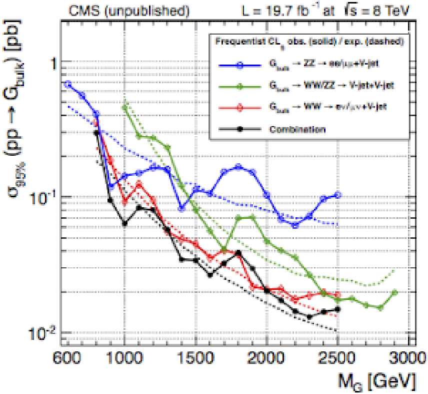

CMS collaboration

Generalized k_t algorithm

- Depends on a parameter p;
- Cluster partons by smallest distance $d_{ij} = \min(z_i^{2p}, z_j^{2p})\theta_{ij}^2$;
- Particular cases:
  - p=0 : C/A algorithm, angular ordered;
  - p=-1 : anti-k_t algorithm;
  - p=1/2 : similar to mass measure.

Non-perturbative effects

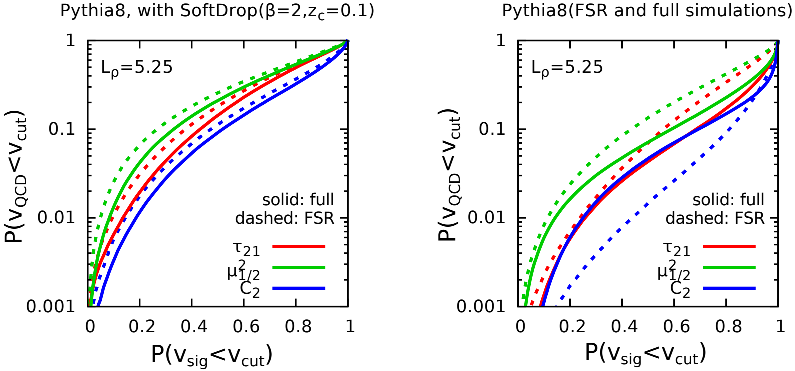

Structure of the results (Signal)

- Decay of a boosted object into a pair $q\bar{q}$ or gg.
- For a signal jet (fixed mass always) + a cut in the shape v:

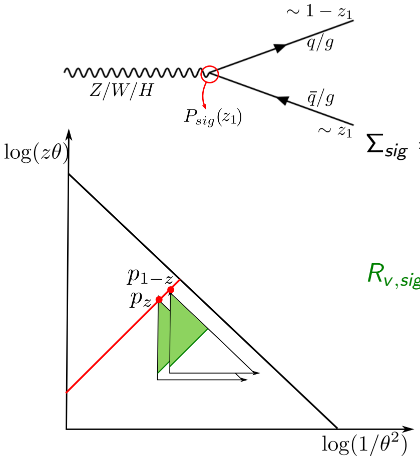

$$\Sigma_{sig} = \int_{\rho}^{1} dz_1 P_{sig}(z_1) e^{-R_{v,sig}(z_1,\rho) - R_{v,sig}(1-z_1,\rho)}$$

$$R_{v,sig}(z_1) = \int_0^1 \frac{d\theta_2^2}{\theta_2^2} \int_0^1 dz_2 P_i(z_2) \frac{\alpha_s}{2\pi} \Theta(v^{sig} > v_{cut})$$